# OUTPUT OF LANDSAT ANALYSIS TO NLP AND CLASSIFICATION OF DATA FOR OKINAWA

Peter ARATHOON,** Seiki KYAN* and Yuuji TANIGUCHI*

**Abstract**

Landsat TM data for Okinawa is analysed by means of training areas representing 8 different types of ground cover which are cloud, water, earth, houses, farm (vegetation other than trees), tarmac (includes concrete), trees and shadow. Statistics for each area are evaluated and output to NLP in the form of average tables, matrices, spectra, level slices and two-dimensional band slices. The original data may also be output to the NLP, (rather than to specialized colour output hardware, as is the case in much more elaborate systems). One band's data is reproduced in eight shades of grey representing relative intensity.

Two classification procedures (6-dimensional minimum distance and 6-dimensional maximum likelihood) are applied, and their results compared. Image output for these is similar to that for original data, except with patterns rather than halftones representing different classes.

## Introduction

### Remote Sensing and Landsat

Remote sensing of the earth's surface involves recording the output of sensitive instruments trained towards it, and processing this to retrieve as much relevant information as possible. In the early days, spectral scanners were used from aircraft, but now many satellites are orbiting the earth, beaming back instrument readings to recording stations on the earth. One such set of satellites is the Landsat series. Landsat-1 tested the Multispectral Scanner, (MSS), from which data were obtained with a ground resolution of 80m in four spectral bands in the visible and infrared.

The two most recent Landsat satellites, Landsat-4 and Landsat-5, launched by NASA in July 1982 and March 1984 respectively, have a new sensor on board called the Thematic Mapper (TM). It has a ground resolution capability of 30m and allows recording of data in seven spectral bands. Table 1 (from ref.5) shows the spectral bands in which the MSS and TM sensors can operate, and Fig.1 (ref.4) shows the same diagrammatically.

Received : October 31, 1986

**Graduate student, Electrical and Information Engineering

*Dept. of Electronics and Information Engineering, Fac. of Eng.

Table 1 : Spectral bands of the MSS and TM

| Spectrum colour | MSS | Wavelength ($\mu$m) | TM | Wavelength ($\mu$m) |
|---|---|---|---|---|
| blue | | | 1 | 0.45 - 0.52 |
| green | 1 | 0.50 - 0.60 | 2 | 0.53 - 0.61 |
| red | 2 | 0.60 - 0.70 | 3 | 0.62 - 0.69 |
| near infrared | 3 | 0.70 - 0.80 | | |
| near infrared | 4 | 0.80 - 1.10 | 4 | 0.78 - 0.90 |
| middle infrared | | | 5 | 1.57 - 1.78 |
| thermal | | | 6 | 10.42 -11.66 |
| middle infrared | | | 7 | 2.10 - 2.35 |

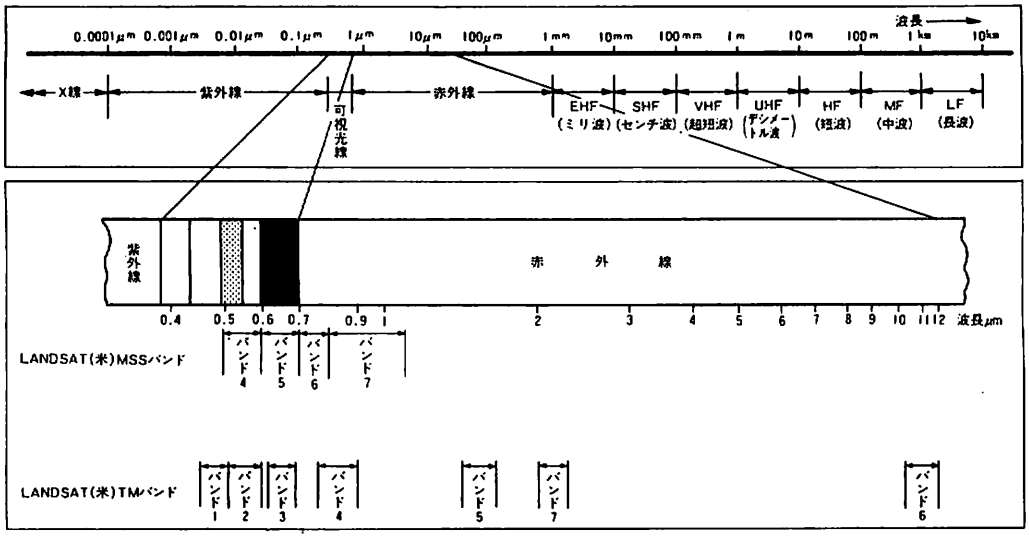


Fig. 1 : Wavelengths of bands for MSS and TM

## Advantages of TM

1. Better spatial resolution, (30m to MSS's 80m).

Particularly necessary for analysis of farm areas in Japan where field sizes are small compared to the U.S.

2. Higher spectral resolution

Narrower spectral bands on the TM allow better differentiation of objects with similar spectral signatures, e.g. different crops, different building materials.

3. Wider spectral range

TM's band－1 is sensitive to shorter wavelengths than MSS's band－1, and is sensitive to the chlorophyll concentration in plants. Bands 5 and 7 reach deeper into the near infrared, both being sensitive to the water content of leaves, with band－5 being sensitive to soil mois-

ture content.

4. Thermal band

TM band－6 is sensitive to a body's temperature, but only has a spatial resolution of 120m as a result of the longer wavelength being received.

Fig.2 (ref.4) shows a graph of the spectral characteristics of broad surface types.

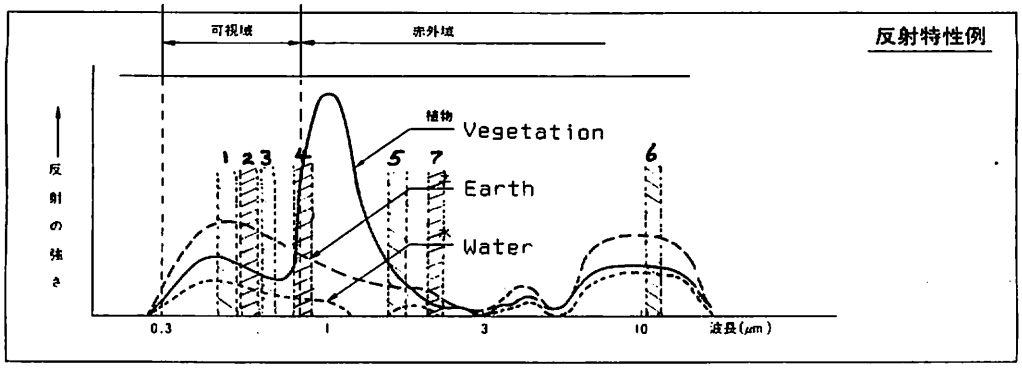


Fig. 2 : Spectral characteristics of surfaces

## Data

TM data was chosen for its advantages as outlined above. The Landsat satellite only passes over a given area once every two weeks approximately, so that in most months only two passes are obtainable, and sometimes only one. When this pass coincides with a holiday or rest day at the receiving station, the data is not recorded. Thus in any year there are a severely restricted number of images available, and out of these the majority are partially or completely dominated by cloud. The most recent fairly acceptable image for Okinawa was for May 9th 1985, and this is the data used in this research. Earlier good images exist, but are thus even less easy to check for accuracy by ground inspection, which is essential even if good maps can be obtained.

Data is in the form of magnetic tapes which can be used as they are or read into a data set in the main computer, (FACOM M340). Recently the latter method has been used. One pixel has 7 bands' data, each of value 0～255, representing the intensity received at the sensor over a certain wavelength range. From west to east there are 4320 pixels, and 2983 lines scan from nearly the northernmost tip of Okinawa to very nearly the southernmost tip. This is the range covered by one Landsat subscene, the smallest unit of Landsat data one can buy. To cover Okinawa completely would thus require 3 or 4 subscenes, which would be prohibitively expensive.

## Output of images to NLP

In the output of an image, the informational content of the original must be preserved in as clear a way as possible. With expensive equipment it is easy to make a colour output of an

image which fulfills these aims. Using black and white it is necessary to make shades of grey serve instead of colour.

In the work described here two sorts of image are desired, one to show the intensity of an image, e.g. when displaying the original image recorded over one wavelength band, and another to show the results of classification of an area into different land – use categories. For these different applications it would be sensible to use a slightly different means of display for each, suited to the purpose in mind.

For the former then, graded shading from say white to black can be used to represent increasing intensities of signal received. This gives an image similar to a photograph. For the latter case of displaying classification results, it becomes more important to be able to see at a glance the category attributed to any one pixel. Whereas the human eye cannot readily distinguish more than a few shades of grey seen in isolation, a pattern is more immediately recognizable, and so patterns rather than halftones are used in images of classification results.

Fig.3 shows a typical output image rendered in eight shades:

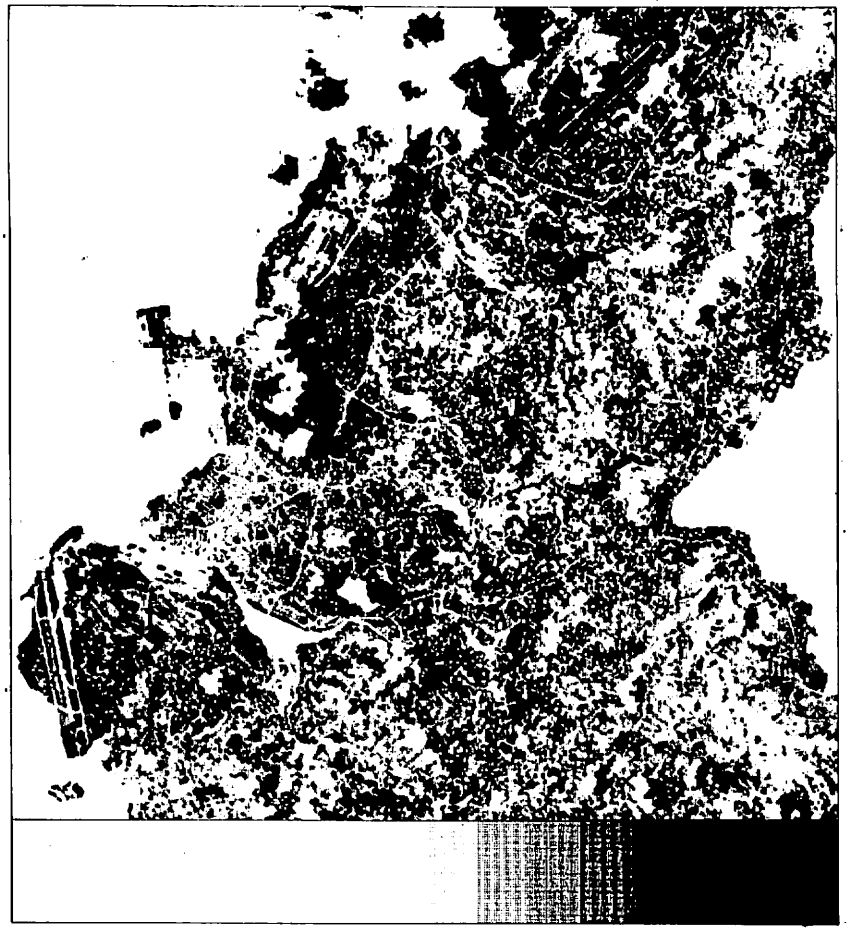

Fig. 3 : Naha, Yonabaru and Ginowan as seen from Landsat
(Band 5)

Classification

This may be broken down into the processes of finding and analysing several "training areas" of a known type of ground cover, e.g. housing areas, woodland, etc., and then applying a method of classification to categorize a large area into these classes. The results must then be compared with reality, and the best approximation picked as a suitable classification method.

a) Training Areas

Eight categories were chosen, and comparison of maps, aerial photographs of Naha and TM data images of the sort described above, allowed the selection of TM data which represents these categories fairly well. Transparent grids were laid over maps, photos and NLP images for ease of comparison. Training areas consist of square areas of ground in most cases, but are supplemented by groups of individual pixels in such classes as Water, which must include river data, in the form of individual pixels for the narrow rivers on Okinawa.

Statistics for each training area were calculated, and were output to the NLP. An example of this analysis is shown in Table 2 below:

Table 2 : Statistics results for Houses training area

STATISTICS
COORDINATES
103 320 6
257 265 15

TOTAL NO OF PIXELS: 261
MEAN AND STANDARD DEVIATION

| | BAND 1 | BAND 2 | BAND 3 | BAND 4 | BAND 5 | BAND 6 | BAND 7 |
|---|---|---|---|---|---|---|---|
| RANGE | 91-164 | 38-84 | 34-101 | 57-121 | 68-169 | 148-154 | 28-92 |
| MEAN | 132.56 | 62.84 | 74.25 | 83.32 | 122.62 | 152.08 | 64.15 |
| S. D. | 14.15 | 7.74 | 11.88 | 11.38 | 13.08 | 1.05 | 9.24 |

VARIANCE COVARIANCE MATRIX

| | BAND 1 | BAND 2 | BAND 3 | BAND 4 | BAND 5 | BAND 6 | BAND 7 |
|---|---|---|---|---|---|---|---|
| BAND 1 | 200.24 | 103.02 | 157.70 | -42.10 | 98.41 | 3.82 | 93.48 |
| BAND 2 | 103.02 | 59.90 | 90.43 | -4.90 | 63.38 | 1.67 | 52.18 |
| BAND 3 | 157.70 | 90.43 | 141.05 | -17.51 | 95.24 | 2.61 | 80.87 |
| BAND 4 | -42.10 | -4.90 | -17.51 | 129.45 | 41.32 | -1.83 | -12.76 |
| BAND 5 | 98.41 | 63.38 | 95.24 | 41.32 | 171.15 | 0.93 | 105.39 |
| BAND 6 | 3.82 | 1.67 | 2.61 | -1.83 | 0.93 | 1.10 | 1.30 |
| BAND 7 | 93.48 | 52.18 | 80.87 | -12.76 | 105.39 | 1.30 | 85.35 |

CORRELATION MATRIX

| | BAND 1 | BAND 2 | BAND 3 | BAND 4 | BAND 5 | BAND 6 | BAND 7 |
|---|---|---|---|---|---|---|---|
| BAND 1 | 1.00 | 0.94 | 0.94 | -0.26 | 0.53 | 0.26 | 0.72 |
| BAND 2 | 0.94 | 1.00 | 0.98 | -0.06 | 0.63 | 0.21 | 0.73 |
| BAND 3 | 0.94 | 0.98 | 1.00 | -0.13 | 0.61 | 0.21 | 0.74 |
| BAND 4 | -0.26 | -0.06 | -0.13 | 1.00 | 0.28 | -0.15 | -0.12 |
| BAND 5 | 0.53 | 0.63 | 0.61 | 0.28 | 1.00 | 0.07 | 0.87 |
| BAND 6 | 0.26 | 0.21 | 0.21 | -0.15 | 0.07 | 1.00 | 0.13 |
| BAND 7 | 0.72 | 0.73 | 0.74 | -0.12 | 0.87 | 0.13 | 1.00 |

25% AND 75% QUARTILES

| | BAND 1 | BAND 2 | BAND 3 | BAND 4 | BAND 5 | BAND 6 | BAND 7 |
|---|---|---|---|---|---|---|---|
| | 121-143 | 56-68 | 65-83 | 73-91 | 114-130 | 151-153 | 58-71 |

As can be seen, the coordinates of the training area are given in triplets of numbers. The first two are the x – y coordinates of the upper – left corner of the training area, and the third number is the length of one side of the chosen square area. Next the total number of pixels within this training area is given, followed by ranges, means and standard deviation for each band. Then come the variance – covariance matrix and correlation matrix, and finally the quartiles for each band, within which 50% of all values lie.

A visual representation of the values of pixels in the training areas for houses and woodland is shown in the level slice graphs below, (Figs. 4 and 5). (The axes for these are explained in the graph for band 6).

From this sort of image one can see the "purity" of the data. If only a single peak exists, then the ground cover is probably very uniform, as is the case with the Trees category. The results for Houses are more widespread, indicating that the ground cover is varied. This reflects the fact that within housing areas there is a certain amount of e. g. vegetation, which will radiate very differently to concrete, the raw material of most Okinawan houses now.

The marked variation in band 3 for the Trees category is perhaps explained by the fact that this is the wavelength region over which vegetation's radiation is particularly strong. Further analysis of this may show that different types of vegetation may be detected based on the variation in radiation intensity over this band.

The next diagram (Fig.6) shows the spectra associated with the eight categories analysed here. They are obtained by plotting the mean intensity against wavelength for each band, (except band 6, the thermal band). Error bars using the quartiles calculated for each category have been omitted for clarity, except for the Trees class.

At the extremes of intensity, it can be seen that clouds and exposed earth radiate strongly at all wavelengths considered here, and that regions of water and shadow are uniformly low radiators. Clouds are bright, which by definition means they absorb and re – emit the sun's radiation strongly. Exposed earth is also a strong radiator for the same reason. As expected, shadow and water regions appear relatively dark, being cooler and less well – illuminated in the former case, these factors lowering their black – body radition curves.

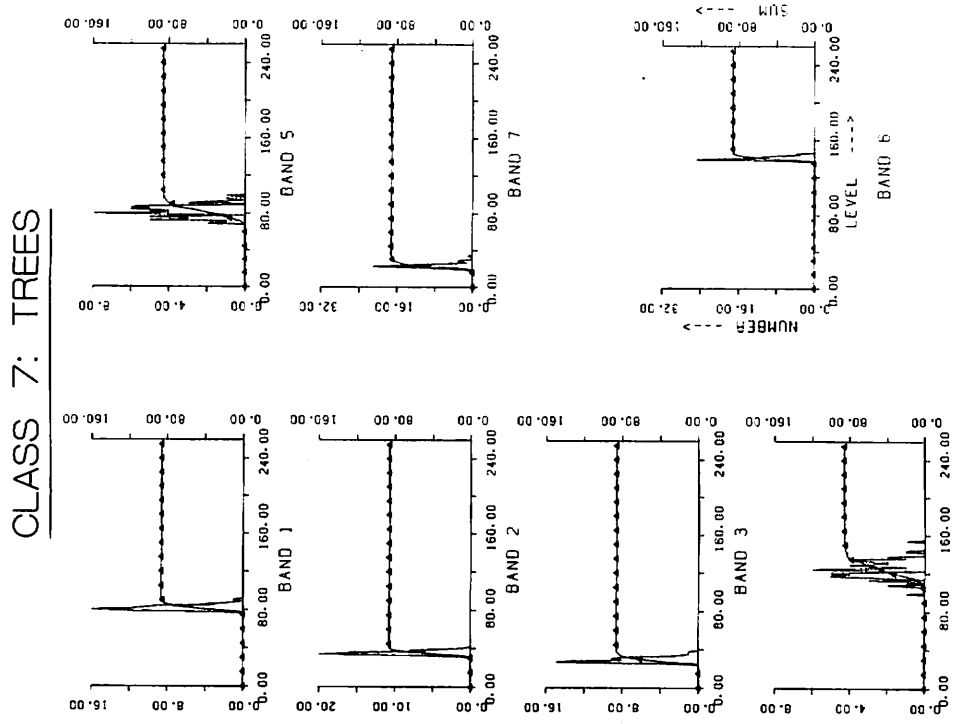


Fig. 5 : Level slices for Trees category

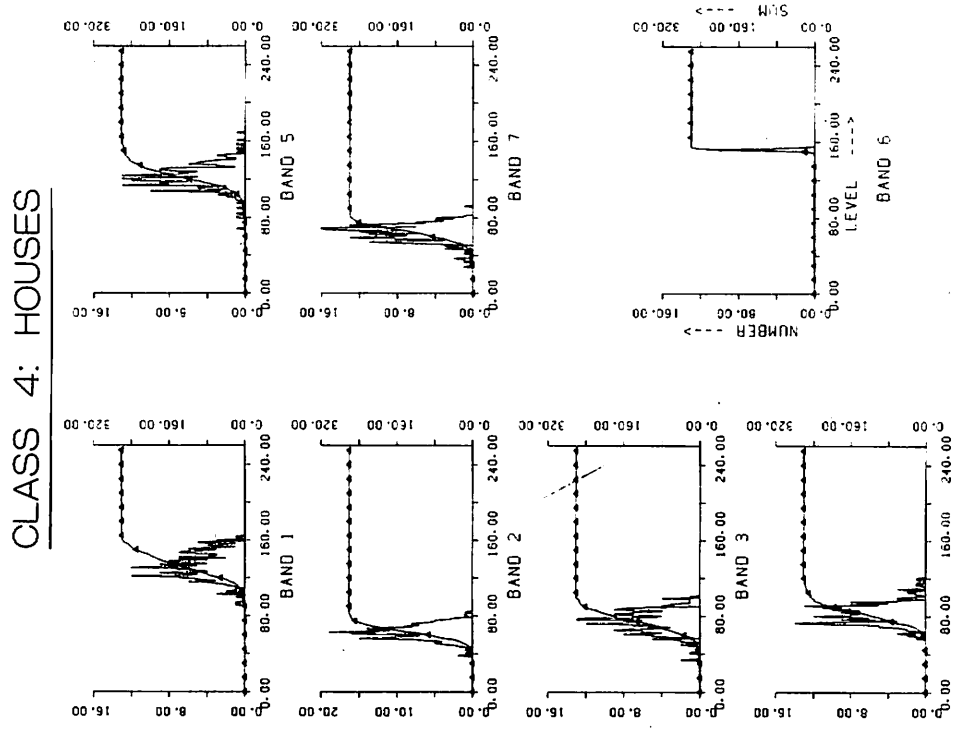


Fig. 4 : Level slices for Houses category

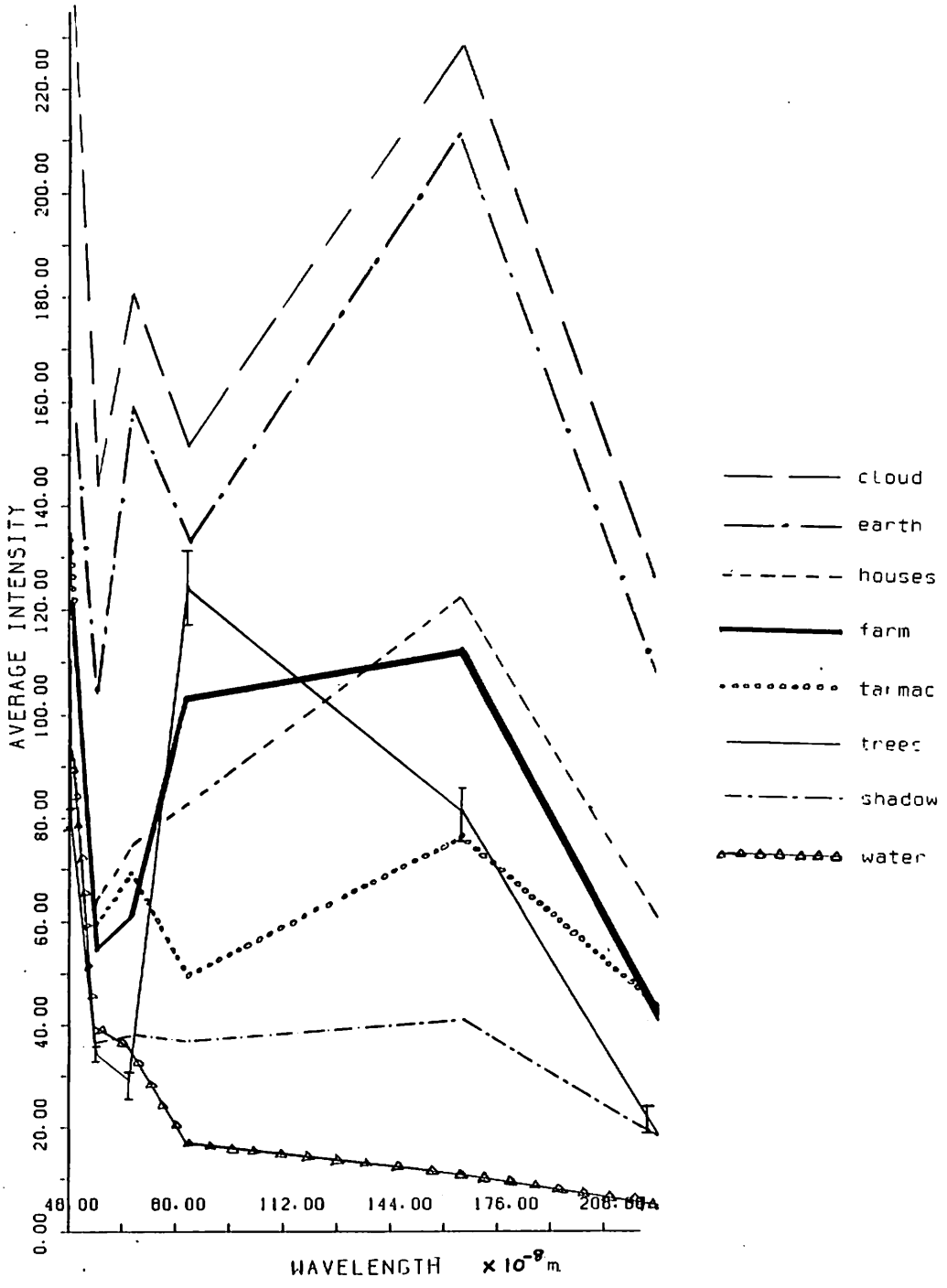


Fig. 6 : Radiation characteristics of the 8 categories.

From the graph of radiation characteristics shown earlier, it can be seen that vegetation may be expected to radiate strongly over bands 4 and 5, and this is reflected in spectra for trees and farmland above. Apart from these two, the only other class to register even a small increase in band 4 radiation over band 3 is houses. This probably reflects the influence of the certain amount of vegetation which will naturally be found in most housing areas.

These spectra show in particular the fact that each class has its own very distinctive pattern of radiation, and it is this which can be utilized to form a means of classification.

For each training area one further result was obtained, 2-dimensional band slices. These plot the values of pixels within the training areas on 2-dimensional graphs, showing the relations existing between pairs of bands. Bands 2 and 3 have been excluded because of their close correlation to band 1 data, (see the correlation coefficient matrix in the statistics table for Houses above). Also intensities received over band 6 have been excluded because of the very small amount of variation observed in this band, and its basically thermal interpretations.

The following graph (Fig.7) shows superposed results for the two training areas previously discussed, Houses and Trees:

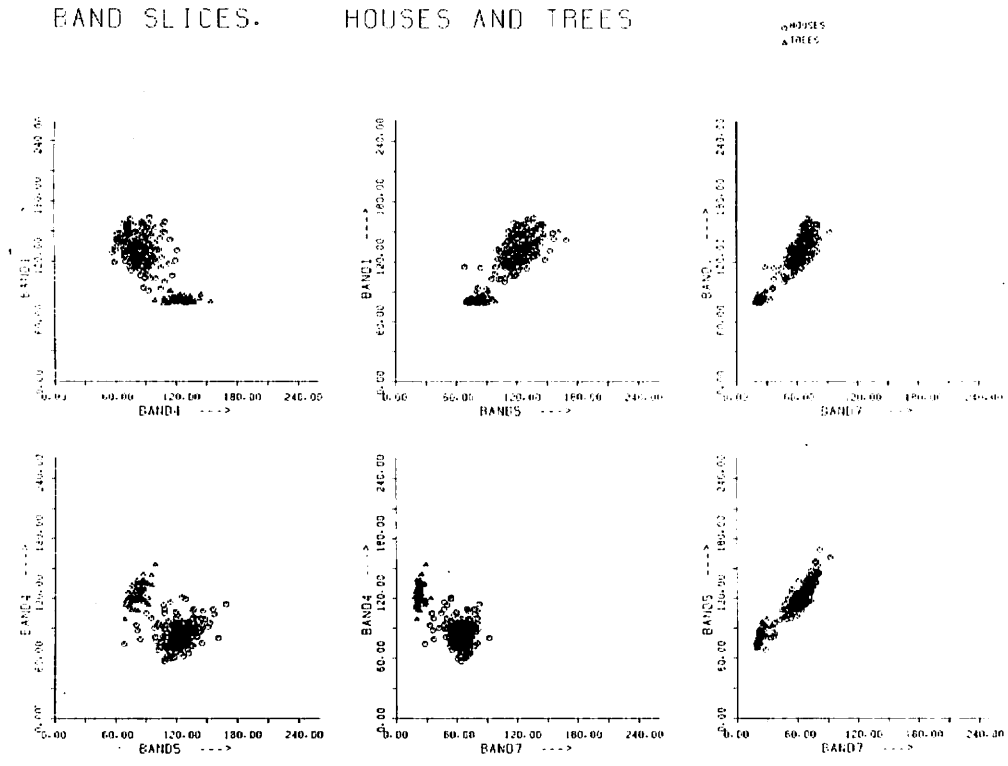


Fig. 7 : Suserposed band slices for houses and trees

It is fairly clear that the two classes are well separated in this diagram, as were their characteristics in the spectra shown previously. This implies that classification into these categories will be relatively problem - free. For classes which overlap to a greater extent, accurate classification will depend a lot more on the method employed.

### b) Methods of classification

The following two methods have been employed, and their results compared:

1) minimum distance method
2) maximum likelihood method

### 1) Minimum distance method

In analysing data from a large area, many pixels will have radiation characteristics very similar to one of the training areas, i. e. for all bands their radiation intensity lies within the range encountered for just one category. Classification for these is simply a matter of putting the pixel in that category. But many pixels will perhaps have one or more bands' data outside this range.

In a two - dimensional case one can determine which class the recalcitrant pixel should be put in by calculating the Pythagorean distance from the pixel's data to the two classes' mean values, and deciding that the appropriate class is simply the nearest class as determined by this method. This would be a two - dimensional minimum distance method, (see example below, Fig. 8 ).

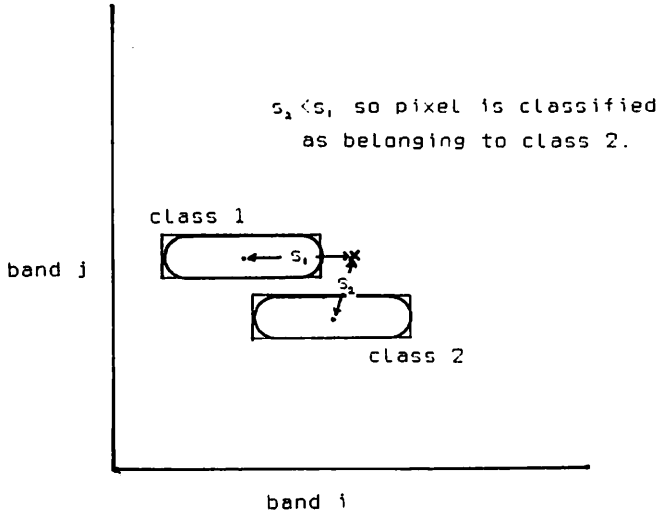


Fig. 8 : Example of minimum distance classification

Loops enclose a fixed proportion of points in each class. Boxes enclose the permitted range of values for each band, and points represent the mean values of both bands for each class.

The classification process is then:

1) put all pixels lying within the above boxes into the appropriate category.

2) put other pixels into the class whose average value they are nearest to.

This method does not use a class's other statistics, (ranges, standard deviations, etc.) for pixels outside the boxes, and so may be expected to be weak. In the example above, the stray pixel would be put in class 2 whereas its characteristics are much more similar to class 1. A more complicated method is obviously necessary to perform this sort of classification.

### 2) Maximum likelihood method

This uses a function which gives the likelihood of a pixel belonging to a certain class k. (The notation and equations used below follow reference (2), pages 314, 315). This function is based on the assumption of a normal distribution of training area pixel values about some mean value for each band and each class.

For n – band data, l categories and m training area pixels in the kth category, the total training area data may be written:

$$x_{ik}=\{x_{ijk}|i=1,\ m;j=1,\ n;k=1,\ l\} \tag{1}$$

The kth category multiple average $\bar{x}_k$ and formula for the variance – covariance matrix $S_k$ are respectively:

$$\bar{x}_k=\left\{x_{jk}=\frac{\sum_{i=1}^{m}x_{ijk}}{m}\,\middle|\,j=1,\ n\right\} \tag{2}$$

$$S_k=\frac{1}{m}\sum_{i=1}^{m}(x_{ik}-\bar{x}_k)\ (x_{ik}-\bar{x}_k)_t \tag{3}$$

For a given pixel data $x=|x_j|\ j=1,\ n|$ (again a multiple value because of there being data for 7 bands for each pirel), the likelihood function is:

$$f_k(x)=\frac{1}{(2\pi)_{n/2}|S_k|^{1/2}}\exp\left\{-\frac{1}{2}d_k^2\right\} \tag{4}$$

Where $|S_k|$ is the determinant of $S_k$, and $d^2_k$ is the Mahalanobis distance

$$d_k^2=(x-\bar{x}_k)^t S_k^{-1}(x-\bar{x}_k) \tag{5}$$

Classification is then into the class k for which $f_k(x)$ is a maximum.

Taking the logarithm of this expression shows that this is equivalent to finding the class k for which the function $g_k(x)$ is a minimum, where

$$g_k(x)=\log|S_k|+(x-\bar{x}_k)^t\cdot S_k^{-1}(x-\bar{x}_k) \tag{6}$$

One further quantity calculated was the interclass distance table, defined by:

$$d_{k1k2}=\sqrt{(\bar{x}_{k2}-\bar{x}_{k1})^t S_{k1}^{-1}(\bar{x}_{k2}-\bar{x}_{k1})} \tag{7}$$

($d_{k_1k_2}$ is interpreted as the "distance" from class $k_1$ to class $k_2$, and is usually different to $d_{k_2k_1}$).

The table of interclass distances is shown below:

Table 3 : Interclass distances

DISTANCE BETWEEN CLASSES

| FROM CLASS : TO CLASS | 1 | 2 | 3 | 4 | 5 | 6 | 7 | 8 |
|---|---|---|---|---|---|---|---|---|
| 1 | 0.0 | 32.67 | 45.69 | 29.60 | 23.96 | 16.69 | 83.97 | 16.13 |
| 2 | 27.34 | 0.0 | 41.78 | 21.42 | 25.65 | 11.58 | 20.89 | 7.15 |
| 3 | 23.38 | 28.97 | 0.0 | 17.37 | 20.00 | 17.43 | 55.08 | 27.08 |
| 4 | 19.79 | 11.70 | 5.69 | 0.0 | 4.35 | 15.51 | 23.20 | 7.27 |
| 5 | 21.48 | 9.63 | 10.18 | 4.29 | 0.0 | 31.81 | 12.62 | 6.48 |
| 6 | 19.10 | 17.93 | 3.52 | 5.14 | 9.90 | 0.0 | 44.47 | 7.26 |
| 7 | 28.60 | 19.63 | 19.93 | 12.13 | 6.44 | 54.86 | 0.0 | 8.16 |
| 8 | 26.17 | 3.84 | 21.44 | 10.81 | 16.64 | 8.89 | 11.87 | 0.0 |

AVERAGE DISTANCE = 23.1550293

### c) Comment on Unclassified class

The Unclassified class contains those pixels which are most different to the eight categories. For the minimum distance case, the distance from these pixels to any class was above a given limit, which was decided arbitrarily to give a final unclassified percentage of about 6 ~ 8%. For the maximum likelihood classification a similar maximum was set for the value of the function $g_k(x)$. If it exceeded this, then the pixel was designated unclassified. This is equivalent to the condition that:

$$d_k \geqq c \qquad (8)$$

where c is a parameter dependant on the class k and pixel value x.

Another better means for determining unclassified pixels is by the inequality:

$$\left| \frac{x_j - \overline{x_{jk}}}{\sigma_{jk}} \right| \geqq \text{DHENS} \qquad (9)$$

where DHENS is an input parameter.

When this is satisfied, the pixel is unclassified.

Comparison of classification methods

The results from the two methods performed are shown below, (Figs. 9 and 10) :

These images show southern Naha in close-up, being magnified four fold from the original 512 × 512 pixel data set. The grid is an option, printed automatically by the program if desired, to help comparison of pixels in detail.

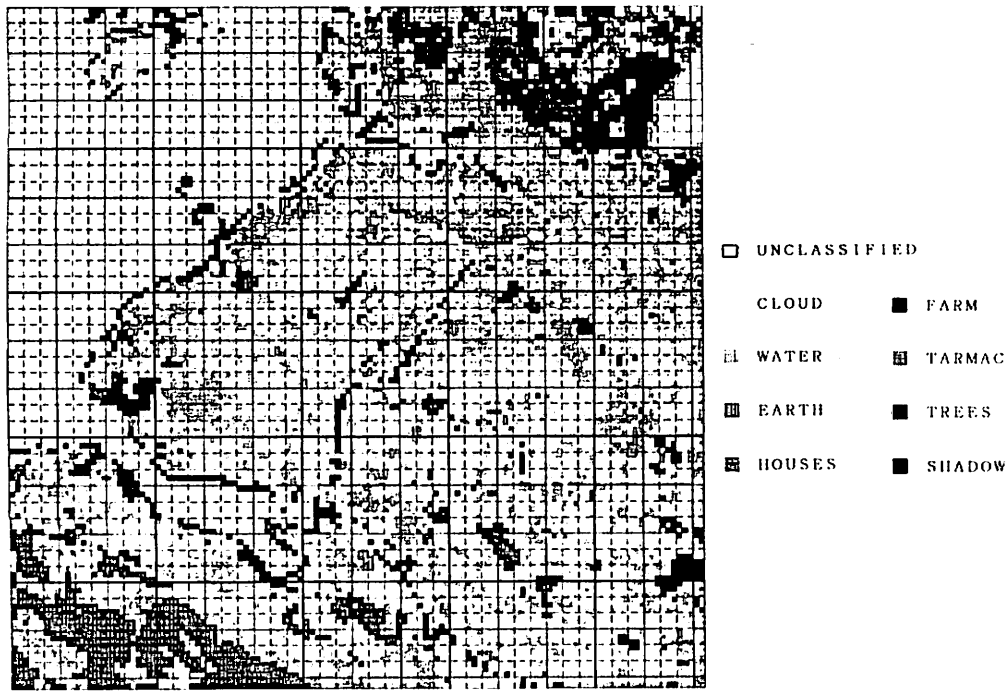


Fig. 9 : Minimum distance classification results for Naha

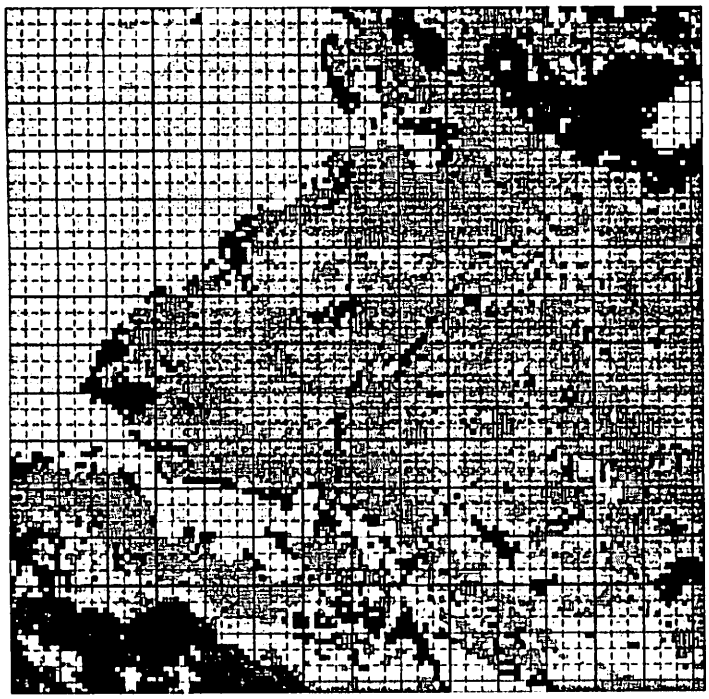

Fig. 10 : Maximum likelihood classification results for Naha

Table 4 : Comparison of results for the whole 512 × 512 image

| | MIN DISTANCE | MAX LIKELIHOOD |
|---|---|---|
| UNCLASSIFIED | 8.17% | 6.18% |
| CLOUD | 0.52% | 1.06% |
| WATER | 26.48% | 26.17% |
| EARTH | 0.59% | 3.07% |
| HOUSES | 25.93% | 23.19% |
| FARM | 21.97% | 27.35% |
| TARMAC | 6.57% | 3.07% |
| TREES | 7.54% | 4.03% |
| SHADOW | 2.24% | 5.89% |

The first comparison is of overall percentages of pixels put into each category. The table below displays the results for the two full 512 × 512 classification results:
Comparing the two methods then, the percentages do not vary greatly, but do show some variation, as is expected. The categories Cloud, Earth, Farm (vegetation other than trees) and Shadow show an increased area for the more accurate maximum likelihood method, at the expense of the Houses, Tarmac and Tree categories. These trends are reflected in the close-up images. Looking at the upper-right corner of each image, there is a light area with a darker area to the left, (west). This represents a cloud (bright) and its shadow, since this data was collected in the morning, with the sun still in the east. Comparison shows that these areas are better classified in Fig.10 than in Fig.9, i.e. that the maximum likelihood results are more precise. The minimum distance results show that much cloud remains unclassified, and other pixels are to be found in the shadow region.

Similarly the light patch at the top left represents an area of thin cloud over sea, thin cloud being notoriously problematic for classification efforts. Fig.10 shows it as a cloud area surrounded by Unclassified and a spot of shadow, but Fig.9 suggests that there are larger areas of Earth, Tarmac and Shadow than of Cloud.

In Fig.9 two lines from the bottom left to top right near the centre of the image may be seen, consisting of unclassified (white) and shadow (black). Also two more straight lines crossing them near top right. One is a main road, and the others are narrow stretches of river with roads on either side. Because the rivers are much narrower than the 30m resolution of a single pixel, the best one can expect perhaps is that the road characteristics will prevail, and in Fig.10 it can be seen that this is what happens, with most pixels becoming classified as tarmac.

Conversely, at bottom left is an area of wasteland, predominantly low scrub, grassland and dirt tracks. In Fig.9 there is a high proportion of tarmac suggested, (horizontal line shading), which dutifully disappears in Fig.10.

In the above and other ways comparison with maps and photographs show that the maximum likelihood method is far superior to the crude minimum distance method, although there remains too high a percentage of shadow. Refinement of the technique should reduce such anomalies in the coming months.

Enhancement

There are many ways to enhance an image using a computer, but so far only a few relatively simple ones have been tried. One involves looking for areas where there is a big difference in adjacent pixel values for one band, and showing this in an image where darker shading represents a bigger difference. This is a sort of differential operation, looking for areas of biggest gradient in radiation intensity. The result shows up such linearly coherent objects as roads fairly clearly. Roads in country areas show up best using band 4, and those in built – up areas using band 5. The image below, (Fig.11), shows the band 4 results:

Fig. 11 : Enhancement results for band 4.

The basic enhancement method is as follows:

For each pixel in the image look for the neighbouring pixel which has the most different value in a given band, and shade the chosen pixel according to the size of this difference.

The same method may be used for multiple bands, in which case all bands are searched and the greatest difference found used to determine the amount of shading. Interpretation of

such results is understandably difficult, but as a means of detecting say roads, this method seems to merit further effort to produce a clearer picture, and eventually perhaps even an approximate road map.

## Conclusions

It has been demonstrated that it is possible to perform analysis of remote sensing data using a non-specialized system, and to produce output of statistical results in the varied form of tables, level slices, spectral graphs and two-dimensional band slices, as well as black and white images represnting original data and results of various classification and enhancement procedures, which adequately convey the inherent information at a fraction of the cost of more specialized display-oriented systems.

In the future it is hoped to increase the accuracy of the present classification, and to improve the image-enhancement techniques to extract more specialized information from the data.

## Acknowledgements

The authors wish to thank senior undergraduate student Tatsuo Shiroma for his assistance in preparing some of the diagrams used in presenting these results at the 39th Electrical conference held at Fukuoka University on 29th-30th September 1986.

## References

1): Image Processing and Analysis,
Japanese Remote Sensing Research Group,
Kyoritsu Publishing. (Japanese language)

2): Computer Processing of Image Data,
Japanese Remote Sensing Research Group,
Kyoritsu Publishing. (Japanese language)

3): Papers of the 8th Remote Sensing Analysts' Seminar, 1985.

4): Satellite-Based Remote Sensing System, page 4,
Remote Sensing Technology Centre.
Toeisha Publishing. (Japanese Language)

5): Adapted from a table by Monique Bernier in a letter (p.7) to:
Remote Sensing in Canada, (Summer 1985)